

On The Birth of Freak Waves Due To The Nonlinear Interaction of Swell and Wind Waves Crossing Each Other With Finite Angle

Yong Jun Cho

Dept. of Civil Engineering, University of Seoul, Seoul, South Korea

Abstract - Lately, strange waves originating from an unknown source even under mild weather conditions have been frequently reported along the coast of South Korea. These waves can be characterized by abnormally high run-up height and unpredictability, and have evoked the imagination of many people. However, how these waves are generated is a very controversial issue within the coastal community of South Korea. In 2006, Shukla numerically showed that extremely high waves of modulating amplitude can be generated when swell and locally generated wind waves cross each other with finite angle, by using a pair of nonlinear cubic Schrodinger Equations. Shukla (2006) also showed that these waves propagate along a line, that evenly dissects the angles formed by the propagating directions of swell and wind waves. Considering that cubic Schrodinger Equations are only applicable for a narrow banded wave train, which is very rare in the ocean field, Shukla (2006)'s work is subject to more severe testing. Based on this rationale, in this study, first we relax the narrow banded assumption, and numerically study the feasibility of the birth of freak waves due to the nonlinear interaction of swell and wind waves crossing each other with finite angle, by using a more robust wave model, the Navier-Stokes equation.

Keywords: Freak waves, Constructive Wave-Wave Interaction, Navier-Stokes Eq., Obliquely Colliding Waves.

I. INTRODUCTION

Since the sudden overtopping of the breakwater at Boryung in 2008, which eventually claimed several lives, freak waves have started to draw attention in the coastal community of South Korea. These waves can be characterized by abnormally high run-up height and unpredictability, which are unusual enough to evoke the imagination of many people. Freak waves are usually known to originate from seemingly nowhere even under mild weather conditions, and have been reported several times along the eastern and southern coast of South Korea.

Even though a great deal of effort has been made over the last several years, no consensus has been reached about under what situations these freak waves can be generated, and it remains an on-going problem. Up to now, several views have been proposed, and many examinations of their validity are still underway. Some people claim that a freak wave is caused by wave energy focusing due to chance superposition of sinusoidal waves with appropriate

phase and spatial orientation, and an increase of wave amplitude occurs randomly. In order for these explanations to be persuasive, the likelihood of an occurrence of freak wave should follow uniform distribution. However, locations of freak wave formation do not seem to be completely random, and in fact there have been several areas which for a long time have held notoriety as freak wave hotbeds such as the coast of South Africa.

Based on the fact that strong currents are a common feature of the region known as freak wave hotbeds, there is also a view following Lavrenov (1998), and White and Fornberg (1998) that a freak wave is the focus of wave energy due to the current moving in the opposite direction of the waves. A rip current that we can frequently observe along the coast can act as the aforementioned counter current. Rip currents decay as they move into deeper waters, and this feature of rip current allows the waves moving against it to draw near to their forerunners and allows for the wave energy to be concentrated in a significantly smaller spatial region than it otherwise would have been. While the preceding situation is perhaps the simplest to understand, this theory is only applicable in the realm of quasi unidirectional waves. Among others, a few researchers claim that edge waves, also known as surf beats, underlying an ever present swell of slowly modulating amplitude in a bound mode can cause unusual run-up after being released from the swell by breaking, since edge waves can be trapped near the coast by refraction (Guza and Thornton, 1981).

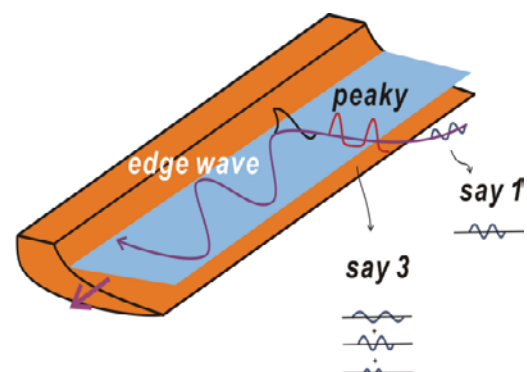


Fig. 1 Edge wave along the coast in trapped mode

Lately, Shukla (2006) devised an innovative idea free from the aforementioned drawback of present theories, and Shukla's work (2006) will be hailed as the beginning of new era in the study of freak wave. Using a pair of cubic nonlinear Schrodinger equations, Shukla (2006) numerically showed that a new instability is evoked when an ever present swell near the shore collides with locally generated wind waves with finite angle less than 62.5°. At the initial phase of instability, a wave packet of abnormally large amplitude is observed to propagate along the direction which evenly dissects the angles formed by propagating directions of swell and wind waves. This new coherent feature inspired Shukla (2006) to name this phenomenon 'constructive instability', which closely mimics every facet of the freak wave. Later, this new instability is saturated by the broadening of wave spectrum, which will enhance dispersion of waves such that the wave system is re-stabilized via phase mixing of the wave envelope, and finally wave amplitude decreases.

In this study, Shukla (2006) first derived a dispersion relationship for colliding waves from cubic nonlinear Schrodinger equations, from which he obtained the growth rate of side disturbance on a horizontal plane, which strikingly differs from that found in the well-known Benjamin Feir instability for one wave system. Shukla (2006) also shows that growth rate depends on the x, y direction wave number of side band disturbance and the angle formed by propagation directions of two waves. Finally, the growth rate of side disturbance is sensitive to the collision angle, and if the collision angle is larger than 65°, the constructive instability disappears.

However, considering the fact that Shukla (2006)'s work relied heavily on nonlinear cubic Schrodinger equation, which is only applicable for narrow banded waves, Shukla (2006)'s work is subject to more severe testing since narrow banded waves are very rare in the ocean field.

Following this rationale, we first relax the narrow band assumption, and proceed to numerically study the feasibility of the formation of freak waves by the collision of two waves in a more general sea state. As a wave driver, we use the Navier-Stokes equation.

II. CURRENT VIEW ON THE FORMATION OF FREAK WAVES

Most of the past studies on freak waves relied heavily on the nonlinear cubic Schrodinger equation due to its ease of being integrable after the inverse scattering transformation method was proposed. Coupled nonlinear cubic Schrodinger equation can be written as

$$i \left(\frac{\partial A}{\partial t} + C_{gx} \frac{\partial A}{\partial x} + C_{gy} \frac{\partial A}{\partial y} \right) + \alpha \frac{\partial^2 A}{\partial x^2} + \beta \frac{\partial^2 A}{\partial y^2} + \gamma \frac{\partial^2 A}{\partial x \partial y} - \xi |A|^2 A - 2\zeta |B|^2 A = 0 \quad (1)$$

$$i \left(\frac{\partial B}{\partial t} + C_{gx} \frac{\partial B}{\partial x} - C_{gy} \frac{\partial B}{\partial y} \right) + \alpha \frac{\partial^2 B}{\partial x^2} + \beta \frac{\partial^2 B}{\partial y^2} + \gamma \frac{\partial^2 B}{\partial x \partial y} - \xi |B|^2 B - 2\zeta |A|^2 B = 0 \quad (2)$$

where A and B are, respectively, the amplitude of slowly varying wave envelopes such that the surface elevation are given by

$$\eta_A = \frac{1}{2} A e^{i(kx+ly-\omega t)} + c.c \quad (3)$$

$$\eta_B = \frac{1}{2} A e^{i(kx-ly-\omega t)} + c.c \quad (4)$$

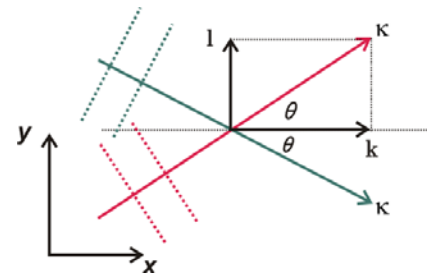


Fig. 2 Definition sketch

In Eq. (1), (2), (3) and (4), c.c denotes complex conjugate, $C_{gx} = \omega_o k / 2\kappa_o$ and $C_{gy} = \omega_o l / 2\kappa_o$ are, respectively, the group velocity component in the x and y direction, $\alpha = \omega_o (2l^2 - k^2) / 8\kappa_o^4$ and $\beta = \omega_o (2k^2 - l^2) / 8\kappa_o^4$ are the group velocity dispersion coefficients, $\xi = \omega_o \kappa_o^2 / 2$ is the nonlinear self-interaction coefficient, and the nonlinear cross interaction coefficient, ζ , is given by

$$\zeta = \omega \left(k^5 - k^3 l^2 - 3kl^4 - 2k^4 \kappa + 2k^2 l^2 \kappa + 2l^4 \kappa \right) / 2\kappa^2 (k - 2\kappa) \quad (5)$$

where ω_o , the angular frequency of the carrier wave, is related to κ_o , the wave number of the carrier wave, by the deep water dispersive relation $\omega_o = \sqrt{g\kappa_o}$.

Considering the facts that in the derivation of Eq. in Eq (1) and (2), perturbation method called multiple scale method and solvability condition were evoked, cubic nonlinear Schrodinger is only applicable to narrow banded waves, which is rare to find in the ocean field.

The stability of Stokes waves have been questioned for many years based on our experience in the laboratory, but

it was Benjamin and Feir (1967) who showed that Stokes waves are unstable to collinear side band disturbances, $\propto e^{i(Kx - \Omega t)}$, the wave number of which are satisfying the following condition

$$\left| \frac{K}{\kappa} \right| = 2\kappa a_o \quad (6)$$

In this case, the side band disturbance grows exponentially with time, and hence is unstable.

Later, this phenomenon becomes to be called as Benjamin and Feir (1967) instability, and plays a crucial role in our understanding how wind wave spectrum evolves. Once Benjamin and Feir (1967) instability gets underway, wave spectrum are getting broadened, and wave groups gets complicated such that we can't find any coherence. In this rationale, Benjamin and Feir (1967) instability are also called as destructive instability or defocusing instability. Sub-harmonic disturbance induced by the wave-wave interaction in the evolution of wind wave spectrum is another name of Benjamin Feir wave. Benney and Roskes (1969) further studied side band disturbances, $\propto e^{i(K_1x + K_2x - \Omega t)}$, which obliquely propagated to the primary Stokes waves. According to Benney and Roskes (1969), in the K_1 and K_2 plane, there are always regions in which the Stokes waves are unstable, and the likelihood of instability is greater for greater water depth. A heuristic explanation of Benjamin and Feir (1967) instability has been given by Lighthill (1978). Consider a Stokes wave train with a slowly modulated envelope. The crests near a peak of the envelope are faster than those on either side of the peak, and, therefore, tend to shorten the waves ahead and lengthen the waves behind. Now, the group velocity in deep water is larger for longer waves. The rate of energy transport is lower in front and higher behind, hence accumulation occurs near the envelope peak, whose height must increase. Similarly, the trough of the envelope will tend to decrease, resulting in instability (see Fig.3).

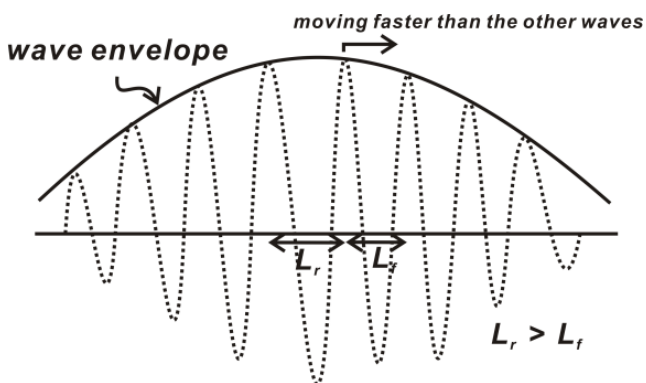


Fig. 3 Stokes waves of slowly modulating amplitude

First, Shukla (2006) notes that crossing sea state is a hotbed for freak waves, and envisions that nonlinear interaction between two colliding waves can be the driving mechanism for freak waves. In this context, Shukla (2006)

introduced a small harmonic perturbation with the wave vector $\mathbf{K} = (\mathbf{K}, L)$ around the equilibrium envelope like

$$A_o + \varepsilon A_1 e^{i(Kx + Ly - \Omega t)}, B_o + \varepsilon B_1 e^{i(Kx + Ly - \Omega t)} \quad (7)$$

, and from Eq. (1) and (2), obtained the nonlinear dispersion relation which can be written as

$$\left[(\Omega - C_{gx} K - C_{gy} L)^2 - \Omega_1^2 \right] \times \left[(\Omega - C_{gx} K + C_{gy} L)^2 - \Omega_2^2 \right] = \Omega_c^4 \quad (8)$$

where

$$\Omega_1^2 = (\alpha K^2 + \beta L^2 - \gamma KL) (\alpha K^2 + \beta L^2 + \gamma KL - 2\xi |A_o|^2)$$

$$\Omega_2^2 = (\alpha K^2 + \beta L^2 + \gamma KL) (\alpha K^2 + \beta L^2 - \gamma KL + 2\xi |B_o|^2)$$

$$\Omega_c^2 = (\alpha K^2 + \beta L^2 + \gamma KL) (\alpha K^2 + \beta L^2 - \gamma KL + 2\xi |B_o|^2)$$

From the above nonlinear dispersion relation, it is obvious that the frequency of perturbation, Ω , depends on the wave amplitude A_o and B_o , the angle between the wave direction and the dichotome θ (see Fig. 4, 5), wave numbers K and L . Soon after, Shukla (2006) numerically solved the nonlinear dispersion relation for Ω by varying K and L , and presented the growth rate of side band disturbances (the imaginary part of Ω) such as follows.

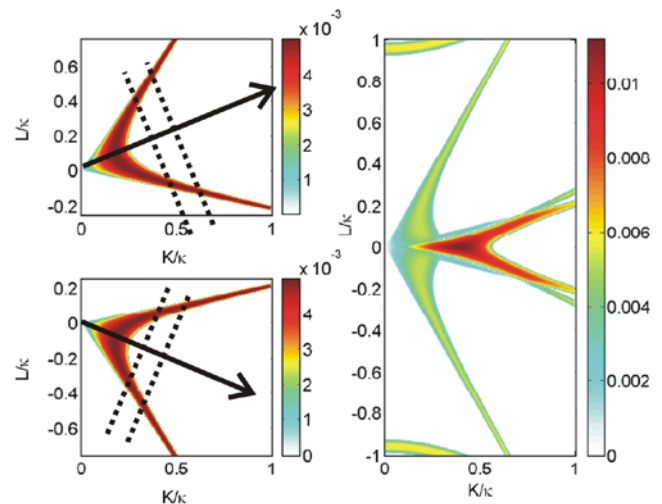


Fig. 4 The normalized growth rate plotted as a function of K and L . The left upper and lower panels show the cases with a single wave, respectively, while the right panel shows the case of interacting waves ($\theta = \pi/8$) [from Shukla et al. (2006)]

Left hand panels correspond to the single wave cases studied by Benney and Roskes (1969), which exhibit the standard Benjamin and Feir (1967) instability. Right hand panels show the cases of two interacting waves. It is obvious that two obliquely colliding waves give rise to a new instability, which is strikingly different from the one

in the single wave cases. These differences can be summarized such as follows.

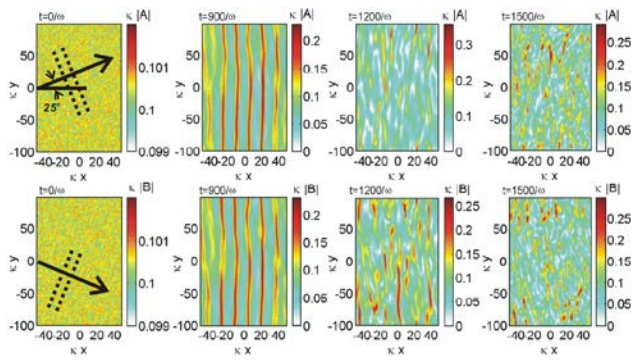


Fig. 5 The interaction between two waves, initially with equal amplitudes $A_o = B_o = 0.1\kappa^{-1}$ and a propagation angle of $\theta = \pi/8$ relative to the dichotome. Added to the initially homogeneous wave envelopes is a low-amplitude noise of order $10^{-3}\kappa^{-1}$ to give a seed to the modulational instability [from Shukla et al. (2006)].

First, for the single wave case, the growth rate has larger values for side band disturbances propagating to the primary waves with more or less $\pm 45^\circ$ whereas for the cases of interacting waves, the growth rate reaches its maxima in the direction of the dichotome, and the maximum growth rate is more than twice as large as the one for single wave cases.

Second, unlike the destructive instability (defocusing instability) where waves dissolved into a wide spectrum of waves as can be found in the Benjamin and Feir instability, in the initial phase of this new instability, two waves are strongly correlated such that wave energy is localized into well defined wave packets of large amplitude which are propagating along the line, which evenly dissect the angles formed by propagating directions of two colliding waves.

Shukla (2006) mentioned that the propagating direction of aforementioned wave packets reflects the facts that the growth rate reaches its maxima in the direction of dichotome.

Third, at later, two waves are decoupled, this new instability will be saturated by the broadening of wave spectrum, which will enhance dispersion of waves such that wave system is re-stabilized via phase mixing of wave envelope, and finally wave amplitude decreases.

These behaviors are very appealing since the new coherent features like the well defined wave packet of large amplitude closely resembles every facets of freak wave, and leads Shukla (2006) to propose that two colliding waves might interact nonlinearly in constructive way to produce large amplitude freak waves in the oceans.

Here, it is worth mentioning that with advent of wave packets, a kurtosis defined as

$$K = \frac{\mu_4}{\mu_2^2}, \quad \mu_i = \int \omega^i S_\zeta(\omega) d\omega$$

would increase, which is also consistent with our experience of freak waves.

III. NUMERICAL MODEL

A. Hydrodynamic model

Wide banded irregular waves can be more accurately described using the more robust wave driver like the Navier Stokes Eq. rather than the nonlinear cubic Schrodinger Eq. In this context, as a wave driver, we used the Navier Stokes Eq., and mass balance Eq., the numerical integration of which is carried out using highly accurate numerical method known as VOF (volume of fluid).

Upon introducing partial area coefficient A_f and partial volume coefficient V_f to express the geometric characteristics of solids in fixed calculation network, we can write the basic eq. such as (see Fig.6)

$$\frac{\partial \tilde{u}}{\partial t} + \frac{1}{V_f} (\tilde{u} A_f \cdot \nabla \tilde{u}) = -\frac{1}{\rho} [\nabla p + \nabla \cdot (\tau A_f)] \quad (9)$$

$$\frac{V_f}{\rho} + \frac{\partial \rho}{\partial t} + \frac{1}{\rho} \nabla \cdot (\rho \tilde{u} A_f) = -\frac{\partial V_f}{\partial t} \quad (10)$$

$$\frac{\partial F}{\partial t} + \frac{1}{V_f} \nabla \cdot (F \tilde{u} A_f) = 0 \quad (11)$$

where ρ denotes fluid density, \tilde{u} denotes the velocity, and F is the volume fraction. If fluid cell is fully immersed, F has a value of 1. If fluid cell is partially immersed, or dried up, it is converged to 0.

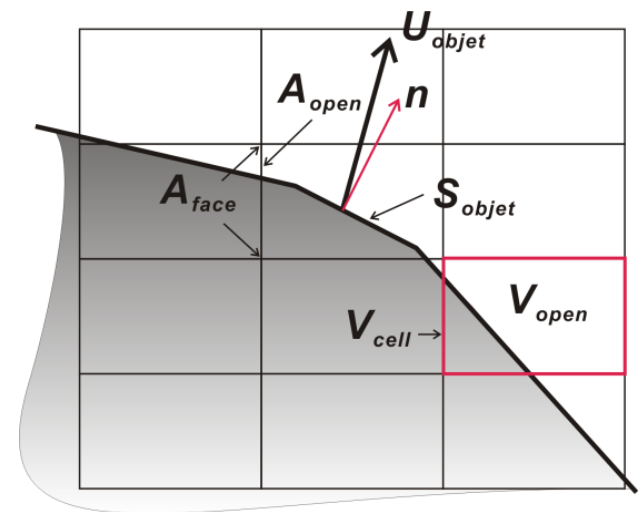


Fig. 6 Schematic showing the calculation of area and volume fraction coefficients, A_f and V_f for solid object (shaded area) imbedded in a rectangular grid.

B. Numerical wave tank

Numerical simulation is implemented on the numerical wave tank of 304m x 248m (see Fig.7). Along the wall of wave tank, we deploy the artificial beach of uniform slope (1:4) in order to minimize the reflection by enforcing wave breaking (see Fig.7).

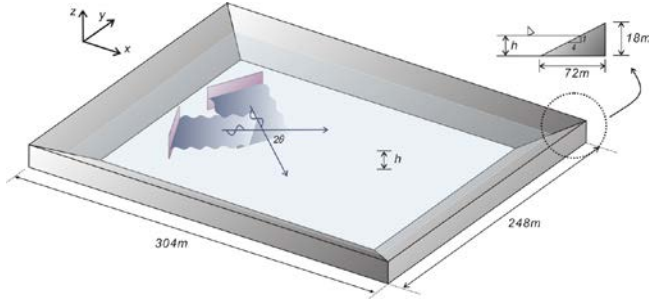


Fig.7 Layout of numerical wave tank

C. Generation of random waves

We numerically generate irregular waves using the random phase method. In the Random Phase Method, wave trains are generated by combining the discrete amplitude wave spectrum corresponding to the target wave energy spectrum with a random phase spectrum synthesized from a random number generator. This yields the Fourier Transform of a time series with the desired discrete power spectrum. The corresponding time series can be obtained by Inverse Fourier Transformation.

The steps of calculating a time series using the Random Phase Method can be summarized as

1. Define a target wave energy density spectrum. In this study, we use the JONSWAP (the Joint North Sea Wave Project) spectrum, which can be written as

$$S_{\zeta}(\omega) = \frac{\alpha_p g^2}{\omega^5} \exp\left(-\frac{5}{4} \frac{\omega_p^4}{\omega^4}\right) \gamma \exp\left[-\frac{(\omega - \omega_p)^2}{2\sigma^2 \omega_p^2}\right] \quad (12)$$

where ω_p is the peak frequency, γ is the peak enhancement parameter, and α_p is the Phillips parameter. Here γ is in the range 1–6 for ocean waves, while α_p is in the range 0.0081–0.1; the values $\gamma = 1$ and $\alpha_p = 0.081$ give the spectrum of fully developed wind seas, while the larger values are observed in water tank experiments. We will use $\alpha_p = 0.025$, $\gamma = 3$, and $\sigma = 0.08$ which are consistent with Shukla (2006). Since the wave spectrum is concentrated around ω_p , we will use $\omega_o = \omega_p$ and $k_o = k_p = \omega_p^2 / g$ in the evaluation of α and β in Eq. (1) and (2).

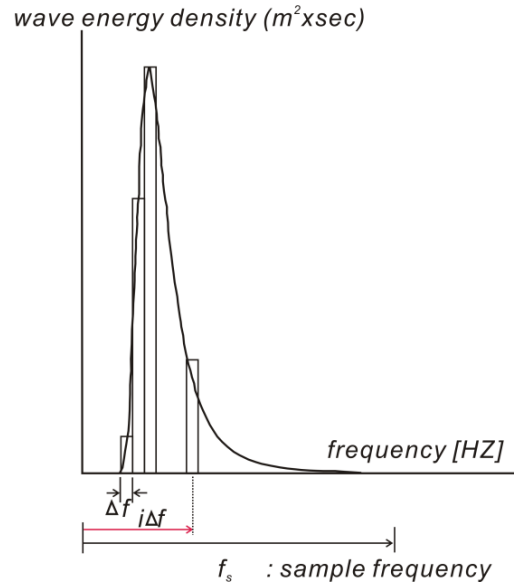


Fig.8 Partition of target wave spectrum

2. Choose the sample frequency, f_s , and the resolution of the spectrum (half the number of Fourier components) N . This yields a frequency domain resolution of $\Delta f = f_s / N$ (see Fig. 8). Calculate the discrete wave energy spectrum $\sigma_{\zeta}(f_i)$

$$\sigma_{\zeta}^2(f_i) = S_{\zeta}(i\Delta f) \times \Delta f, \quad f_i = i\Delta f, \quad i = 1, 2, \dots, N \quad (13)$$

3. Determine the discrete paddle-displacement energy spectrum. The far field transfer function for small amplitude regular waves was given by Biesel (1951) in the following form for piston wave paddles:

$$\frac{H}{S_o} = \frac{2 \sinh^2 kh}{\sinh kh \cos kh + kh}$$

Utilizing the above transfer function, the discrete paddle-displacement energy spectrum $\sigma_x^2(f_i)$ can be written as

$$\sigma_x^2(f_i) = \frac{\sigma_{\zeta}^2(f_i)}{\left(\frac{2 \sinh^2 kh}{\sinh kh \cos kh + kh}\right)^2} \quad (14)$$

Where H is the wave height, S_o is the stroke of the piston, k is the wave number, and h denotes a water depth.

4. Calculate the N complex Fourier coefficients $C(f_i) = A(f_i) + iB(f_i)$ by picking a random phase, $\psi(f_i)$, between 0 and 2π for all frequencies smaller than the Nyquist frequency, $f_n = f_s/2$, where A and B are given by

$$A(f_i) = \sqrt{\frac{\sigma_x^2(f_i)}{2}} \cos(\psi(f_i)) \quad (15)$$

$$B(f_i) = \sqrt{\frac{\sigma_x^2(f_i)}{2}} \sin(\psi(f_i)) \quad (16)$$

5. Mirror the N Fourier components into the Nyquist frequency f_N in order to obtain a hermitian Fourier Transform:

$$C_{N+i} = C_{N-i+1}^*, \quad i = 1, 2, \dots, N$$

Where upper-script * denotes complex conjugate.

6. Apply the inverse Fourier Transform to $C(f_i)$ and calculate the time series of the control signal for the wave paddle such as follows

$$X(t) = \int C(f) e^{-i2\pi ft} df \quad (17)$$

Fig.9 demonstrates sample time series of randomly simulated wave paddle displacement.

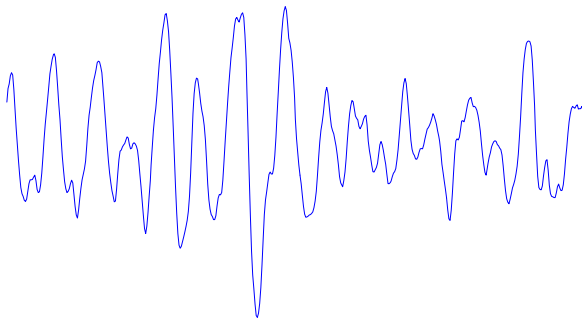


Fig.9 Time series of randomly simulated wave paddle displacement

IV. NUMERICAL RESULTS

To test the feasibility of formation of freak waves by two obliquely colliding waves like swell and local wind waves in more general sea state, we carry out numerical simulation by relaxing the narrow banded assumption. We assume both of two random wave trains follow JONSWAP (the Joint North Sea Wave Project) spectrum, peak period and significant wave height of which are 4s, 9m, respectively.

A. Normally colliding case, $2\theta = 90^\circ$

It was Phillips (1960) who introduced seemingly complicated concept called nonlinear resonance wave-wave interaction. As it is indispensable for our understanding of how wind wave spectrum evolves, it seems like that nonlinear resonance wave-wave interactions play a crucial role for our understanding of propagating direction of wave packet. Hence, here, we erect to briefly summarize these concepts.

In a case that three primary free waves are involved in the interaction, after Taylor series expansion with respect to $z=0$, perturbation terms like $e^{k_1 \pm k_2 \pm k_3}$, $e^{\omega_1 \pm \omega_2 \pm \omega_3}$ are generated in free surface dynamic boundary condition. For

resonance among a tetrad of wave numbers, the following conditions

$$k_1 \pm k_2 \pm k_3 \pm k_4 = 0 \quad (18)$$

$$\omega_1 \pm \omega_2 \pm \omega_3 \pm \omega_4 = 0, \quad \omega_r = \sqrt{gk_r}$$

must be or nearly satisfied. For many sign combinations, no solutions are possible, but it can be shown that there do exist solution sets to (Phillips, 1977).

$$k_1 + k_2 = k_3 + k_4, \quad \omega_1 + \omega_2 = \omega_3 + \omega_4, \quad \omega_r = \sqrt{gk_r} \quad (19)$$

Using a geometrical construction by Simmons (1969), we can depict solution sets satisfying Eq. (19) such as follows

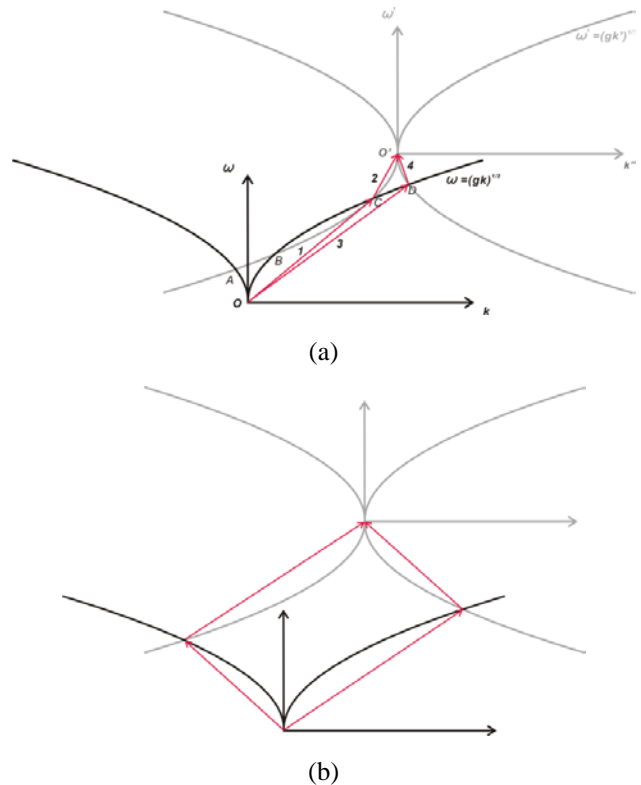


Fig. 10 Example of resonance diagram in wave number, frequency space illustrating the four components that satisfy the resonance condition in Eq. (18)

where the dispersion relation $\omega = \sqrt{gk}$ is represented by trumpet shaped surface in three dimensional spaces. For the configuration shown in Fig. 8a, the original surface from O and the one from O' intersect at four points. The vectors to any two of them from O, and from them to O' evidently specify a set that satisfies Eq. (19). In three dimensions, the intersection of the two surfaces defines two closed loops; as all wave numbers are more or less of equal magnitude, O' is moved vertically and two loops (see Fig 8b) merge when two surfaces just touch, opening out into a single loop as the contact disappears. A projection of the family of the loops onto the wave number plane is shown in Fig. 9, specifying the sets of wave numbers for surface waves capable of undergoing resonant interactions (Phillips, 1976).

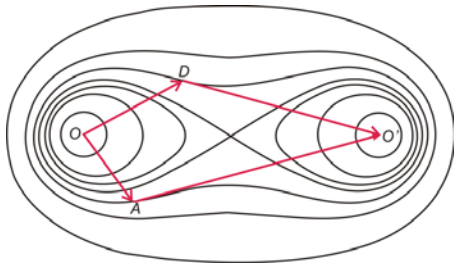


Fig. 11 The family of curves in the wave number plane defined by the resonance conditions in Eq. (19)

In the meanwhile, Longuet-Higgins (1962) suggested a convenient case for experimental study to test aforementioned resonant wave interactions. Later, Longuet-Higgins and Smith (1966) mechanically generated two mutually perpendicular waves along adjacent walls of a square tank, and succeed to measure the 4th component waves (k_1 in Fig. 11) to initially zero, and grow with increasing distance across the tank as a result of the interaction. In this particular set of resonance condition, two of the primary wave numbers are coincident. In this case, the resonance conditions in Eq. (19) reduce to

$$k_1 + k_2 = 2k_3, \quad \omega_1 + \omega_2 = 2\omega_3, \quad \omega_r = \sqrt{gk_r} \quad (20)$$

where k_2 and k_3 are mutually perpendicular. Again, under geometrical construction by Simmons (1969), this resonance condition can be depicted such as

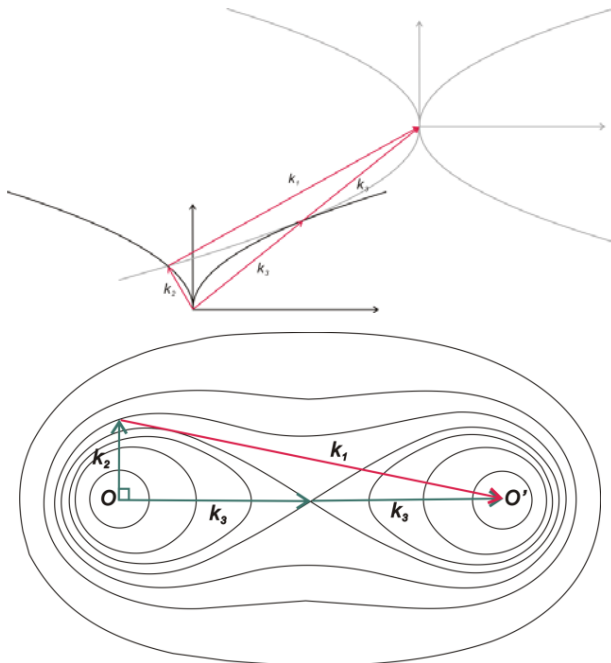


Fig. 10 Resonance conditions suggested by Longuet-Higgins (1962b)

. Noting that the resonance condition envisioned by Longuet-Higgins (1962) can provide a very challenging task for the verification of numerical model proposed in this study, we carry out numerical simulation using similar wave conditions with Longuet-Higgins and Smith (1966).

We generate two mutually perpendicular monochromatic waves using two wave paddles which are squarely deployed. In Fig. 12, we plot snapshot of numerically simulated wave field at 48.753 s.

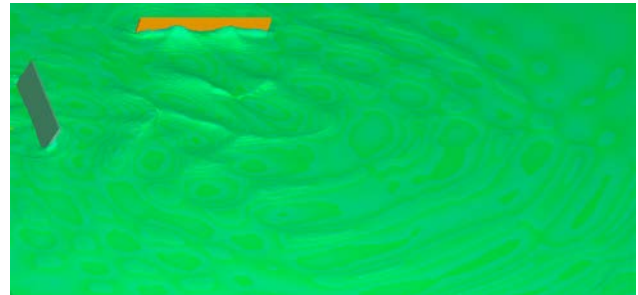
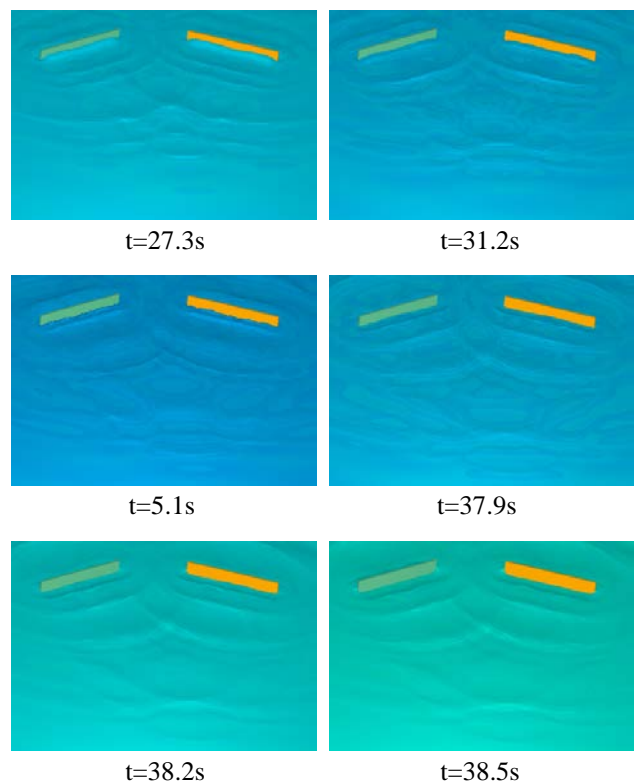


Fig.12 Snapshot of numerically simulated wave field where two waves are colliding with an angle of 90°

B. Obliquely colliding case, $2\theta = 45^\circ$

Following Shukla (2006), constructive instability disappears when the collision angle is larger than 70.6°, but no explanation of its physical background was mentioned. Following this rationale and to unveil the underlying mechanism of constructive instability, we carry out the numerical simulation by adjusting the collision angle as 45°, and keep the wave condition and water depth same as in the previous case.

In Fig. 13, we plot sequential snapshots of numerically simulated wave field from $t=27.3s$ to 48.s. At $t=42.9, 43.2, 43.8, 44.2s$, it is clearly visible that a wave packet of huge amplitude is propagating along the direction which evenly dissects the angles formed by propagating directions of two waves.



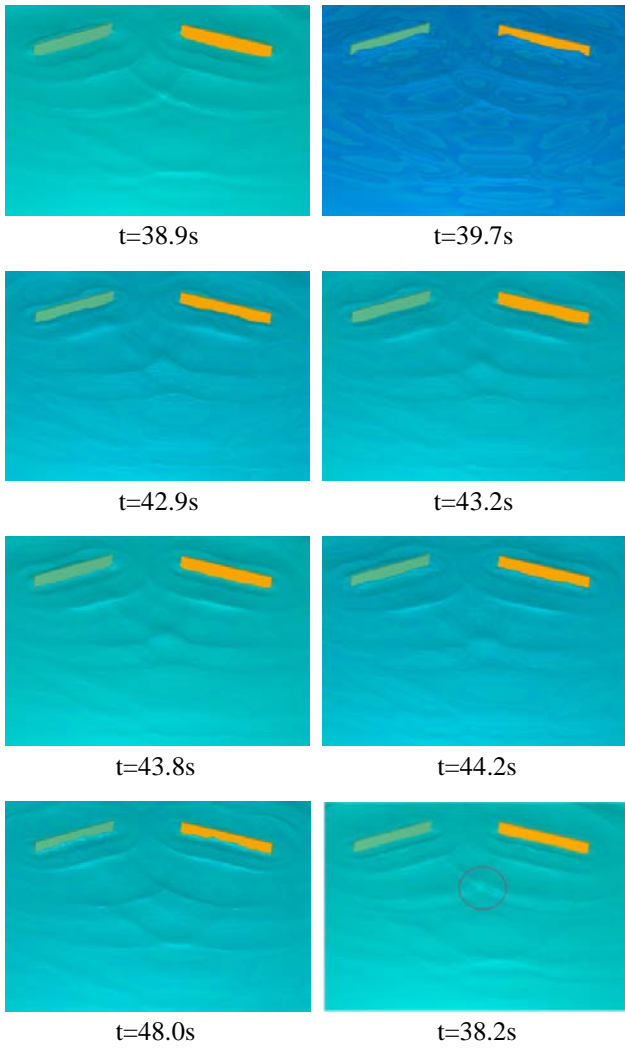
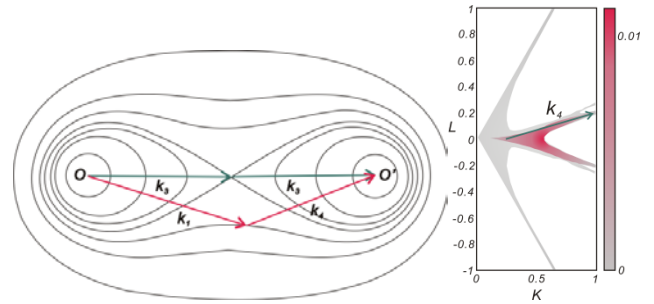
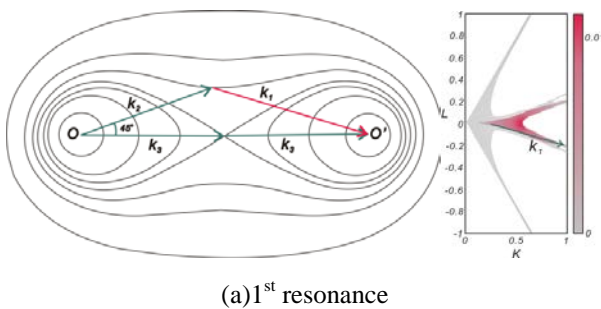


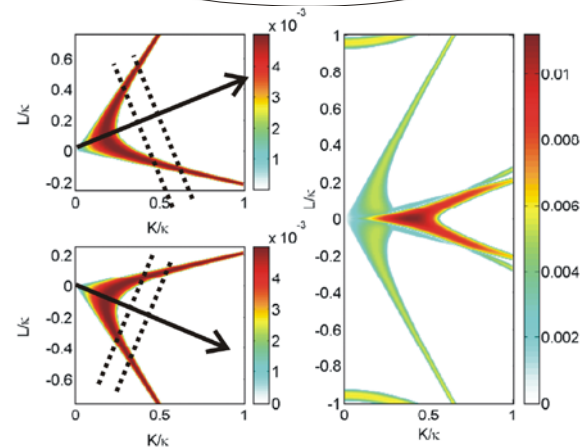
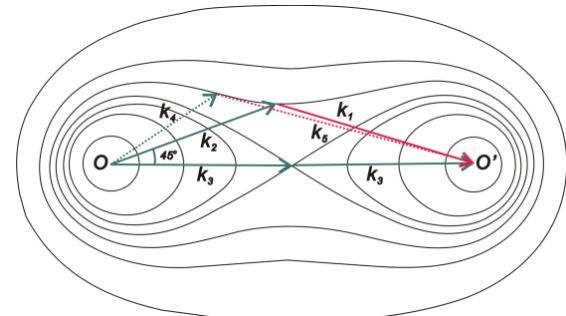
Fig.13 Numerically simulated wave field

C. On the propagation direction of freak wave

Even though Shukla's work (2006) put very valuable step stone to solve the mystery of freak wave, Shukla (2006) did not provide any physical explanation why wave packet in the initial phase of constructive instability is heading to dichotome. In this section, we are trying to answer this question of great engineering value. Now, we have enough grounds to believe that nonlinear resonance wave-wave interaction is underlying mechanism of the new instability occurring in crossing sea state. Following a geometrical construction by Simmons (1969), resonance condition in obliquely colliding case in 4.2 can be depicted such as the following



(b) 2nd resonance



(c) 3rd resonance

Fig.14 the propagation direction of freak wave depicted in the resonance diagram.

That is, first, the interaction between k_2 and $2k_3$ evokes k_1 , which corresponds to the lower branch in the instability diagram by Shukla (2006). Hereafter we call it the 1st resonance. As soon as k_1 is emerged from the 1st resonance, the interaction between k_1 and $2k_3$ gets under way, and results in k_4 which corresponds to the upper branch in the Shukla's (2006) instability diagram. With the multiple resonance interactions occurring in queue, more wave energy are transferred to the wave component aligned with the x axis. With the aforementioned resonance sequence in mind, we can explain why a wave packet of abnormally large amplitude heading to the dichotome is emerging at the initial phase of instability. Here, it is worth mentioning that a set of four wave modes that do not satisfy the resonance condition in equation (20) may still undergo significant interaction since the small phase mismatch can be offset by amplitude dispersion. Hence the growth rate of large value in Fig. 13 is widely

distributed when the wave numbers are small, and shrinks as wave numbers are getting larger, and interaction are more easily triggered when wave numbers of similar magnitude.

VI. CONCLUSION

Despite of a great deal of effort, it seems like that we don't have enough information to answer the simple question like under what situation freak waves can be triggered, yet. Considering the fact that nowadays, freak waves are more frequently observed, mystery about the formation of freak waves is an overdue task partly hampered by our addiction to a simplified wave driver like the Boussinesq equation which often falls short in the explanation of highly nonlinear phenomenon like strong wave-wave interaction.

Lately, Shukla (2006) extended the stability analysis similar with the one used in the classical stability analysis of Stokes waves exposed to collinear side band disturbances, to two obliquely colliding wave trains based on the nonlinear cubic Schrodinger equation, and observed new instability equipped with many features that can't be found in the conventional instability.

Usually, the spectra of waves that go through instability are getting broadened, and wave groups get complicated such that we can't find any coherence. Hence, up to now, instability is known to be destructive as in Benjamin and Feir (1967) instability.

However, at the initial phase of this new instability, a wave packet of abnormally large amplitude is observed to propagate along the direction which evenly dissects the angles formed by propagating directions of two wave trains. This new coherent feature inspired Shukla (2006) to name this phenomenon 'constructive instability', which closely mimics every facet of the freak wave.

It is needless to say that Shukla's work (2006) put very valuable step stone to solve the mystery of freak wave, but it is also true that they left huge room to improve since Shukla's work (2006) is only limited to narrow banded waves which is rare in the ocean field and Shukla (2006) did not provide any physical explanation why wave packet in the initial phase of constructive instability is heading to dichotome.

Following this rationale, we first relax the narrow band assumption, and proceed to numerically study the feasibility of the formation of freak waves by the collision of two waves in a more general sea state. As a wave driver, we use the Navier Stokes equation.

In the numerically simulated wave field, we can successfully observe a wave packet of abnormally large amplitude to propagate along the direction which evenly dissects the angles formed by propagating directions of two wave trains. We also show why the maximum growth

rate is more than twice as large as the one for single wave cases, and growth rate reaches its maxima in the direction of dichotome by using a geometrical construction by Simmons (1969). It turns out that the multiple resonance interactions occurring in queue play a crucial role in the so called constructive instability.

REFERENCES

- [1] Benjamin, T. B. and Feir, J. E. (1967), "The Disintegration of Wave Trains in Deep Water", Part 1. *J. Fluid Mech.* 27, 417-430.
- [2] Benney, D.J. and Roskes, G.D. (1969), "Wave Instabilities", *Studies Appl. Math* 48: 377-385
- [3] Biesel (1951), "Les Apparails Generateurs de Houle en Laboratoire". *La Houille Blanche*, Vol. 6, nos. 2,4 et 5.
- [4] Guza, R.T., and Thornton, E.B. (1981), 'Wave Set-Up on A Natural Beach', *Journal of Geophysical Research: Oceans* (1978-2012) Volume 86, Issue C5
- [5] Lavrenov, I. V. (1998), "Mathematical Modelling of Wind Waves at Non-Uniform Ocean (in Russian)", *Gidrometeor'zdat*.
- [6] Lighthill. M.J. (1978), "Waves in Fluids", Cambridge University Press, London.
- [7] Longuet-Higgins (1962), "Resonant Interactions Between Two Trains of Gravity Waves", *Journal of Fluid Mechanics*, Vol. 12, Issue 3, pp. 321-332.
- [8] Longuet-Higgins, M. S., Smith, N. D. (1966), "An Experiment on Third-order Resonant Wave Interactions". *J. Fluid Mech.* 25: 417-35
- [9] Phillips, O. M. (1976), "The Dynamics of the Upper Ocean", Cambridge University Press.
- [10] Shukla, P. K. (2006), "Instability and Evolution of Nonlinearly Interacting Water Waves", *Phys. Rev. Lett.* 97, 094501
- [11] Simmons, W. F. (1969), "A Variational Method for Weak Resonant Wave Interactions", *Proceedings of the Royal Society A*.
- [12] White, B. S., and Fornberg, B. (1998), "On the Chance of Freak Waves At Sea", *J. Fluid Mech.*, 355, pp. 113-138.